**Supplementing Information**

# $H_2O_2$-activated mitochondria-targeting photosensitizer for fluorescence imaging-guided combination photodynamic and radiotherapy

Qiufen Tian, [a, #] Zifan Zhu, [a, #] Yun Feng,[a] Shirui Zhao,[a] Hui Lin, [b, *] Wen Zhang, [a, *] and Zhiai Xu [a, *]

[a] School of Chemistry and Molecular Engineering, East China Normal University, Shanghai 200241, China.

[b] Gastroenterology department, Shanghai Jing'an District Zhabei Central Hospital, Shanghai 200072, China.

[#] Equally contributed.

E-mail: wzhang@chem.ecnu.edu.cn; niliuh@163.com; zaxu@chem.ecnu.edu.cn. Tel&Fax: +86-2154340053

## Experimental

**Materials and reagents**.

4-Bromomethylphenylboronic acid pinacol ester was purchased from Macklin Biochemical

Co., Ltd (Shanghai, China). 3-(4,5-Dimethyl-2-thiazolyl)-2,5-diphenyl-2H-tetrazolium bromide (MTT) was purchased from Beyotime Biotechnology Co. Sodium nitrite ($NaNO_2$), sodium nitrate ($NaNO_3$), hydrogen peroxide ($H_2O_2$), sodium hypochlorite (NaClO), ferrous chloride ($FeCl_2$), potassium superoxide ($KO_2$), calcium chloride ($CaCl_2$), magnesium chloride ($MgCl_2$), t-butyl hydroperoxide (TBHP), and concentrated nitric acid were purchased from Sinopharm Chemical Reagent Co Ltd (Shanghai, China). Fetal bovine serum (FBS) was purchased from Thermo Fisher Scientific (Waltham, USA), and cell culture medium (DMEM) was purchased from Yuanpei Biotechnology Co. Other organic solvents were purchased from Titan Technology Co (Shanghai, China).

**Instruments and equipment**

Cary 60 spectrophotometer was used to detect UV-vis absorption and FS5 spectro-fluorophotometer was used to detect fluorescence spectra, respectively (Agilent Technologies, USA). MTT assay was done by Cytation 3.0 Multi-Mode Reader (BioTek Instruments, Inc., USA). Cryogenic centrifuge 5427 R was used for ultrafiltration concentration of nanomicelles (Eppendorf AG, Germany). Nanomicelles were prepared with JY92-IIN ultrasonic cell pulveriser (Xinzhi Biotechnology Co., China). The morphology and particle size of the micelles were characterized by HT7700 transmission electron microscope (Hitachi High-Technologies, Inc. Japan) and ZEN3700 particle sizer (Malvern Instruments Inc., UK), respectively. NMR spectra were collected on Bruker Advance spectrometer (500 MHz or 600 MHz, Germany). High resolution mass spectrometer (HR-MS) was acquired with Agilent 1290-6545XT mass spectrometer. Confocal Laser Scanning Microscopy (CLSM) images were acquired with a Nikon-A 1R confocal scanning microscope (Nikon Instrument Co., Shanghai, China). In vivo fluorescence images were observed by Caliper IVIS Lumina I in vivo imaging system (PerkinElmer, Inc., USA). Colocalization analyses were calculated by ImageJ.

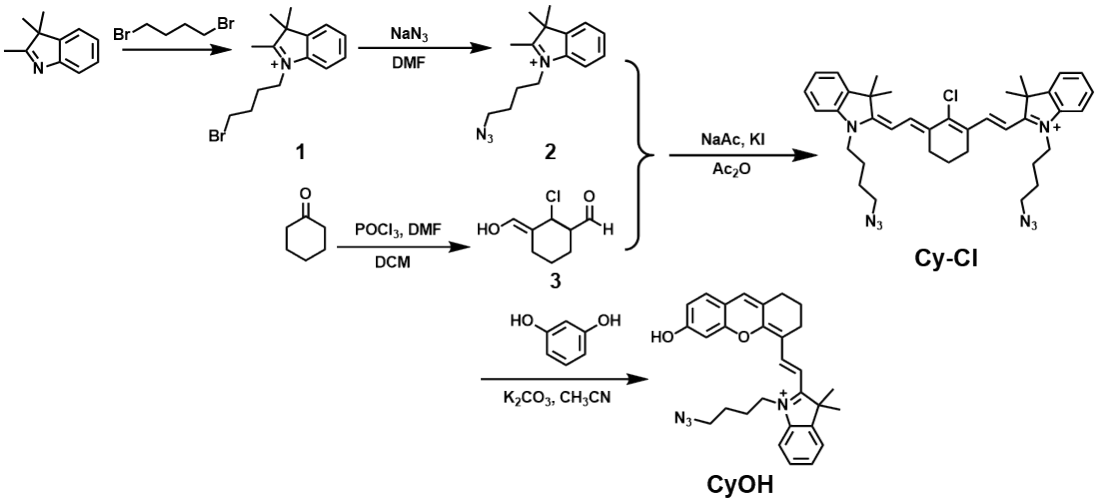


**Synthesis of compound 1**

2,3,3-Trimethylindole (6.4 g, 40.0 mmol) and 1,4-dibromobutane (16.0 g, 80.0 mmol) were added to a 100 mL round-bottomed flask and reacted at 90 °C for 2 h until large amounts of purple solid were precipitated from solution. The solid was washed with acetone, the color changed from purple to white, and compound 1 could be obtained without further purification.

**Synthesis of compound 2**

Compound 1 (2.9 g, 10.0 mmol) was dissolved in anhydrous dimethylformamide (DMF) with stirring, followed by the addition of sodium azide (1.9 g, 30.0 mmol), and the reaction was stirred at 50 °C for 12 h to obtain a red liquid. DMF was evaporated and diluted with DCM, neutralized with saturated $NaHCO_3$ and washed several times with deionized water. The organic layers were combined, dried over anhydrous sodium sulfate and concentrated to give the crude product compound 2.

**Synthesis of compound 3**

Under the $N_2$ atmosphere and 0℃ ice bath, $POCl_3$ (30.0 mL, 116.0 mmol) was slowly added into 72.0 mL (DCM: DMF = 1:1, V/V) and stirred for 30 min, then cyclohexanone (9.0 mL, 96.0 mmol) was added, and the reaction was refluxed at 80 ℃ for 6 h. At the end of the reaction, the reaction solution was added to ice water. The yellow solid was precipitated overnight, washed with water and petroleum ether, and dried to obtain compound 3 without further purification.

**Synthesis of Cy-Cl**

Compound 2 (1.5 g, 5.8 mmol), compound 3 (0.5 g, 2.9 mmol) and sodium acetate (0.2 g, 2.9 mmol) were dissolved in 40 mL of acetic anhydride and KI (0.5 g, 2.9 mmol) was added. The mixture was stirred under $N_2$ at 90 °C for 4 h. After the reaction, the acetic anhydride was evaporated, and the residue was extracted three times by water and saturated $NaHCO_3$, respectively. The crude product was purified by column chromatography on silica gel (DCM:$CH_3OH$ = 50:1) to give the product Cy-Cl (1.0 g, 70%). **$^1$H NMR** (500 MHz, $CDCl_3$) δ 8.12 (d, *J* = 14.0 Hz, 2H), 7.42 - 7.36 (m, 4H), 7.26 - 7.24 (m, 2H), 7.19 (d, *J* = 8.0 Hz, 2H), 6.31 (d, *J* = 14.0 Hz, 2H), 4.30 (t, *J* = 7.5 Hz, 2H), 3.46 (t, *J* = 6.5 Hz, 2H), 2.79 (t, *J* = 6.5 Hz, 2H), 2.01 - 1.93 (m, 6H), 1.86 - 1.78 (m, 4H), 1.72 (s, 12H). **$^{13}$C NMR** (126 MHz, $CDCl_3$) δ 172.2, 150.6, 144.4, 141.9, 140.8, 128.8, 127.6, 125.3, 122.2, 110.9, 101.3, 50.9, 49.2, 44.3, 28.1, 26.7, 26.1, 24.6, 20.6. HRMS (ESI): calcd for $C_{38}H_{46}ClN_8^+$ [M]: m/z 649.3528; found, 649.3512.

**Synthesis of CyOH**

Potassium carbonate (0.5 g, 3.4 mmol) and meso-diphenol (0.4 g, 3.4 mmol) were dissolved in $CH_3CN$ at 55 °C and stirred for 15 min, and then Cy-Cl (0.75 g, 1.15 mmol) was fully dissolved and added to the reaction solution. After the reaction has been completed, the residue was diluted with $CH_2Cl_2$ and washed three times with water and saturated $NaHCO_3$. The organic layer was dried over anhydrous sodium sulfate and concentrated under reduced pressure. The crude product was further purified by column chromatography on silica gel (DCM:$CH_3OH$ = 30:1) to give the product CyOH (0.35 g, 60%). **$^1$H NMR** (500 MHz, $CDCl_3$) δ 8.15 (d, *J* = 13.5 Hz, 1H), 7.35 (s, 1H), 7.31 (t, *J* = 8.0 Hz, 2H), 7.23 (d, *J* = 9.0 Hz, 1H), 7.09 (t, *J* = 7.5 Hz, 1H), 6.87 – 6.84 (m, 2H), 6.73 (s, 1H), 5.70 (d, *J* = 13.5 Hz, 1H), 3.88 (t, *J* = 7.5 Hz, 2H), 2.69 (t, *J* = 6.0 Hz, 2H), 2.63 (d, *J* = 6.0 Hz, 2H), 1.92 – 1.86 (m, 8H), 1.68 (s, 6H). **$^{13}$C NMR** (151 MHz, $CDCl_3$) δ 161.0, 158.3, 143.4, 140.0, 139.9, 135.1, 129.7, 128.3, 125.1, 123.6, 123.1, 122.2, 118.4, 115.9, 108.6, 103.3, 95.7, 50.9, 48.0, 43.0, 29.6, 28.6, 28.1, 26.3, 24.4, 24.0, 22.6, 21.1. HRMS (ESI): calcd for $C_{29}H_{31}N_4O_2^+$ [M]: m/z 467.2442; found, 467.2449.

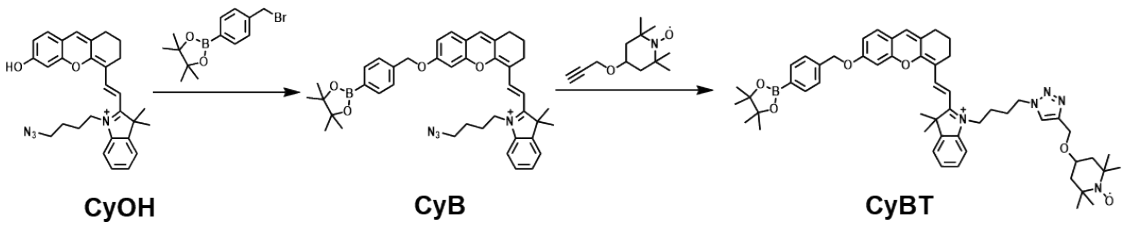


**Synthesis of CyB**

4-Bromomethylphenylboronic acid pinacol ester (120 mg, 0.4 mmol), potassium carbonate (85.0 mg, 0.6 mmol) and potassium iodide (40.0 mg, 0.25 mmol) were dissolved in acetonitrile under the protection of $N_2$ and stirred vigorously at 40 °C for 30 min. CyOH (93.0 mg, 0.2 mmol) was added to the reaction mixture and the temperature was heated to 60 °C, refluxed for 12 hours. After cooling to room temperature, the solvent was evaporated and dissolved with DCM, and extracted three times with water and saturated $NaHCO_3$. The organic phases were combined, dried over anhydrous sodium sulfate and concentrated under reduced pressure. The crude product was further purified by column chromatography on silica gel (DCM:$CH_3OH$ = 20:1) to give the purer product CyB (80 mg, 70%). **$^1$H NMR** (500 MHz, $CDCl_3$) δ8.61 (d, *J* = 14.7 Hz, 1H), 7.87 (d, *J* = 8.3 Hz, 2H), 7.49 (dd, *J* = 15.0, 7.4 Hz, 5H), 7.40 (t, *J* = 7.3 Hz, 1H), 7.33 (d, *J* = 8.7 Hz, 1H), 7.15 (s, 1H), 6.93 (d, *J* = 8.6 Hz, 1H), 6.85 (s, 1H), 6.76 (d, *J* = 14.8 Hz, 1H), 5.24 (s, 2H), 4.71 (s, 2H), 3.48 (s, 2H), 2.90 (s, 2H), 2.73 (s, 2H), 2.04 – 1.98 (m, 2H), 1.97 – 1.88 (m, 4H), 1.78 (s, 6H), 1.34 (s, 12H). **$^{13}$C NMR** (151 MHz, CDCl3) δ 177.2, 161.9, 161.5, 154.2, 146.0, 141.7, 141.4, 138.9, 135.2, 133.2, 129.4, 128.7, 127.8, 127.2, 126.6, 122.4, 116.0, 115.6, 113.6, 112.9, 104.9, 102.0, 84.0, 70.9, 50.9, 50.5, 45.9, 29.2, 28.3, 26.1, 25.1, 25.0, 24.8, 24.8, 20.3. HRMS (ESI): calcd for $C_{42}H_{48}BN_4O_4^+$, [M]: m/z 683.3763; found, 683.3785.

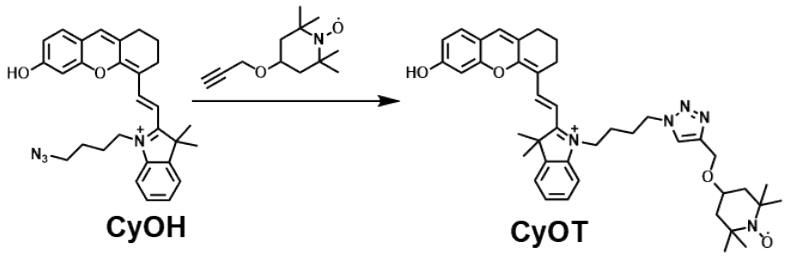


**Synthesis of CyOT**

CyOH (50 mg, 0.1 mmol), 4-alkynylpropoxy-TEMPO (42 mg, 0.2 mmol) were dissolved in a

mixed solution of $CHCl_3/CH_3OH/H_2O$ (6:0.5:0.5, v/v/v) under the protection of $N_2$ and stirred for 15 min, then triethylamine (TEA) and CuI (20 mg. 0.1 mmol) were added, the reaction was carried out at room temperature. After the reaction, the solution was diluted with DCM and extracted three times with water and saturated $NaHCO_3$. The organic phases were combined, dried over anhydrous sodium sulfate and concentrated under reduced pressure. The crude product was purified by column chromatography on silica gel (DCM:$CH_3OH$ = 18:1) to give the purer product CyOT (30 mg, 60%). HRMS (ESI): calcd for $C_{41}H_{51}N_5O_4^{\bullet+}$, [M]: m/z 677.3936; found, 677.3923.

**Optical properties and measurements of CyBT**

CyBT and CyOT were dissolved in PBS solution (10 mM, pH 7.4) to obtain a probe solution of 10 μM, and the corresponding absorption and fluorescence spectra were measured ($\lambda_{ex}$ = 680 nm).

**Fluorescence response of CyBT to $H_2O_2$**

1.8 mg of CyBT was dissolved into 2 mL of DMF to prepare stock solution of 1mM for subsequent testing. And it was diluted with PBS solution (10 mM, pH 7.4) to a final concentration of 10 μM, and then $H_2O_2$ (100 μM) was added, shaken and incubated at 37 °C for different time (0-60 min). In another group, different concentrations of $H_2O_2$ (0-100 μM) were added to PBS solution containing CyBT, shaken and incubated at 37 °C for 60 min. The fluorescence spectra of all the samples were examined.

For the determination of the detection limit, CyBT (10 μM) was incubated with various concentrations of $H_2O_2$ (1-100 μM) for 60 min before recording the emission profiles. The detection limit was calculated with the following equation:

$$\text{Detection limit} = 3\sigma / k$$

**Statistical analysis**

The standard deviation (SD) was calculated as follows:

$$SD = \sqrt{\frac{\sum_{i=1}^{n}(x_i - \bar{x})^2}{n}}$$

$x_i$ represents the value of each data point, $\bar{x}$ represents the arithmetic mean of the data, $n$ represents the number of data points.

**Selectivity and anti-interference property of CyBT**

1 mM of CyBT was diluted with PBS solution, and 500 μM of $K^+$, $Ca^{2+}$, $Mg^{2+}$, $Cu^{2+}$, $Na^+$, $Cl^-$, and $SO_4^{2-}$, 200 μM of GSH, Cys, $ONOO^-$, $^1O_2$, •OH, TBHP, $O_2^{\bullet -}$, $ClO^-$, $NO_2^-$, and $H_2O_2$ (100 μM) were added separately, and incubated at 37°C for 60 min to collect the fluorescence spectra of all samples.

**Effect of pH on CyBT response towards $H_2O_2$**

The fluorescence spectra of CyBT in response to $H_2O_2$ in PBS solution at different pH (4.0 ~ 10.0) were examined separately. In addition, the fluorescence intensities of CyOH and CyOT were tested at the same pH conditions, and the values at 710 nm were recorded.

**Detection of singlet oxygen**

Singlet oxygen generation of CyBT was initially evaluated using a molecule, 1,4-diphenylbenzofuran (DPBF) in dimethyl sulfoxide (DMSO). CyBT (1 mM) was diluted with DMSO to a final concentration of 10 μM CyBT. After that, DBPF was added to DMSO solution to maintain its absorbance of 415 nm at approximately 1.0. Besides, the experiments were carried out in the dark, and then the solution was exposed to 655 nm laser (80 mW/cm$^2$) multiple times. After every irradiation, the absorbance of the DPBF was recorded.

**Response mechanism**

HRMS-ESI verified the molecular weight change after incubation of CyBT (10 μM) with $H_2O_2$ (100 μM).

**Cell cytotoxicity**

The toxicity of probe CyBT and micellar NPs-CyBT's on HeLa cells was tested using MTT assay. Cells were spread into 96-well plates and grown to the required density ($1\times10^4$) for the experiment. A series of concentration gradients of CyBT and micellar NPs-CyBT solutions were prepared and added to the medium-containing cells and incubated for 12 h. The cells were further incubated for 4 h after adding the prepared MTT reagent. Finally, the original liquid

was removed, DMSO was added, shaken well, and the absorption value at 490 nm was determined.

**Fluorescence imaging of exogenous $H_2O_2$ in HeLa cells**

HeLa cells were inoculated at a suitable density ($1\times10^4$) and cultured in confocal quadruple dishes. Subsequently, one group of HeLa cells pre-incubated with CyBT (10 μM) was taken and co-incubated with 0, 40, 80, and 120 μM $H_2O_2$ for 1 h; the other group of HeLa cells pre-incubated with NPs-CyBT (10 μM) was taken and co-incubated with 0, 30, 60, 90, and 120 μM $H_2O_2$ for 1 h. The cells were imaged using confocal laser scanning microscopy ($\lambda_{ex}$ = 647/57 nm, $\lambda_{em}$ = 794/160 nm).

**Fluorescence imaging of endogenous $H_2O_2$ in HeLa cells**

Under the same culture conditions, one group of HeLa cells preincubated with CyBT (10 μM) was washed three times and replaced with fresh medium; the other group of HeLa cells preincubated with NPs-CyBT (10 μM) was washed three times, replaced with fresh medium, and placed under an irradiator with X-rays at an irradiation strength of 8 Gy for 4 min, and incubated for different time (0, 2, 3, 4 h). After then, the cells were washed with PBS and imaged using confocal laser scanning microscopy ($\lambda_{ex}$ = 647/57 nm, $\lambda_{em}$ = 794/160 nm).

**Detection of intracellular reactive oxygen species upon X-ray irradiation**

HeLa cells pre-incubated with NPs-CyBT (10 μM) were irradiated with X-Ray at an irradiation intensity of 8 Gy, and then left for 0 h, 1 h, and 2 h, respectively; the original medium was removed, washed several times, and incubated with DCFH-DA (10 μM) for 20 min. Finally, the original liquid was removed and washed three times with PBS, and then confocal imaging was performed ($\lambda_{ex}$ = 647/57 nm, $\lambda_{em}$ = 794/160 nm).

**Cell survival upon laser and X-ray irradiation**

MTT assay:

The lethality of probe CyBT and micellar NPs-CyBT upon 655 nm laser and X-Ray irradiation on HeLa cells was firstly tested by MTT assay. For the X-ray combined photodynamic group, cells pre-cultured with NPs-CyBT were first irradiated with 8 Gy, then irradiated with 100

mW/cm$^2$ laser for 3 minutes, and finally incubated for another 2 h and washed with PBS; for the only X-Ray irradiation group, cells pre-incubated with NPs-CyBT were irradiated at a radiation intensity of 8 Gy, incubated for 4 h, and then finally MTT was added to further incubate the cells for 4 h. Subsequently, DMSO was added and shaken well. The absorbance of each well was determined with cytation 3 cell imaging multi-mode reader.

Live-dead staining:

HeLa cells were seeded in 48-well plates and cultured to the desired density ($1\times10^4$). The photodynamic group: cells were first incubated with CyBT (10 μM) or NPs-CyBT (10 μM) for 40 min, replaced with new medium, irradiated with a 655 nm laser at 100 mW/cm$^2$ for 0, 3, 6 and 9 min, and put back to the incubator for 2 h. The radiation and photodynamic group: cells were incubated with CyBT (10 μM) and NPs-CyBT (10 μM) for 40 min and irradiated with X-ray at an irradiance of 8 Gy. After that, the cells were then irradiated with a 655 nm laser at 100 mW/cm$^2$ for 0, 3, 6, 9 min and placed back into the incubator for 2 h. And then the cells were stained with Calcein-AM/PI live/dead cell double staining kit for 20 min, and washed for imaging after removing the original working solution.

**Animal experiment**

Female BALB/c-nu-nu mice weighing basically 18-20 g were purchased from the Experiment Centre of East China Normal University (ECNU). The mice were housed and experimented in a SPF-grade environment, and the experiments were conducted in strict compliance with the Institutional Animal Care and Use Committee for Animal Experiments of ECNU (IACUC).

**Fluorescence imaging of HeLa tumor-bearing mice**

HeLa cells ($3\times10^6$ cells/each) were injected subcutaneously into the right hind limb of mice, and when the tumor volume of the mice grew to nearly 100 mm$^3$, the mice were randomly divided into three groups. 100 μL of PBS, NPs-CyBT (2 mg/kg), and NPs-CyBT + X-ray were injected intra-tumorally and treated, and subsequently IVIS imaging was performed ($\lambda_{ex}$ = 680 nm, $\lambda_{em}$ = 710 nm).

**Tumor treatment in vivo**

HeLa cells ($3\times10^6$ cells/each) was injected subcutaneously into the right hind limb of mice, and

when the tumour volume of the mice grew to nearly 100 $mm^3$, the mice were randomly divided into five groups. The following treatment regimens were used: 1) PBS, 2) PBS + X-Ray, 3) NPs-CyBT, 4) NPs-CyBT + Laser, and 5) NPs-CyBT + X-Ray + Laser. The mice were immobilized in lead buckets prior to intratumoral administration, exposing the tumor location only. Subsequently, mice were irradiated with X-ray at a radiation intensity of 4 Gy, and photodynamic therapy at 655 nm (150 $mW/cm^2$) was performed at 24 and 48 h time points, and the administration and treatment regimen were repeated for three times in a cycle of 4 days, and body weights and tumor volumes of the mice were recorded every 2 days, and the mice were euthanized on day 21. After the experiment, tumors were dissected out from mice and tumors photographs and weights of each group were recorded. The volume of mouse tumor was calculated according to the formula:

$$V = 0.5 \times a \times b^2$$

"V" represents the volume of the mouse tumor, "a" represents the longest diameter of the tumor area, and "b" represents the diameter of the tumor perpendicular to "a".

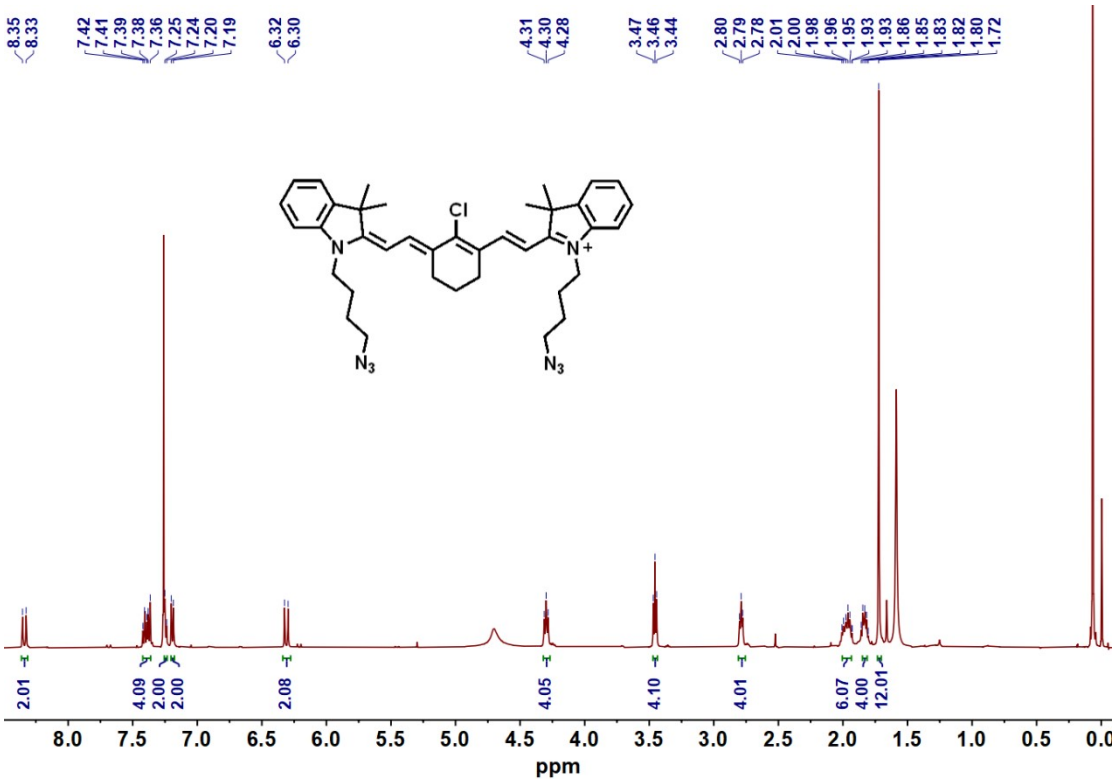


**Fig. S1** $^{1}$H NMR spectrum of Cy-Cl in $CDCl_3$.

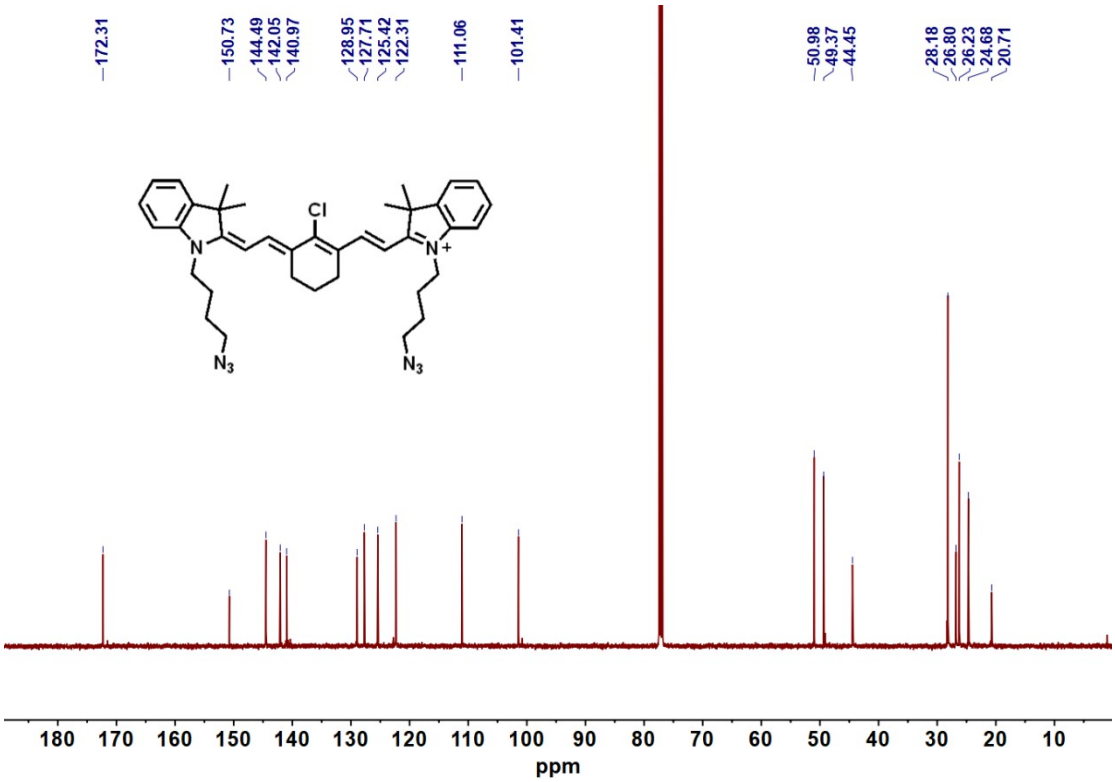


**Fig. S2** $^{13}$C NMR of Cy-Cl in $CDCl_3$.

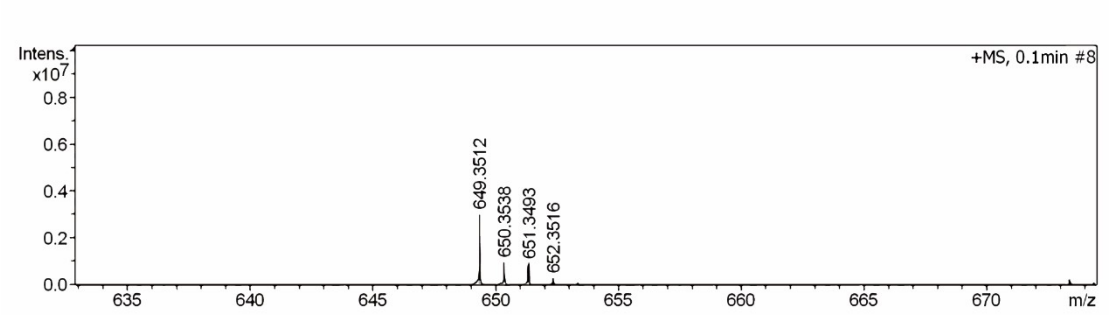


| # | m/z | Res. | S/N | I | I % | FWHM |
|---|---|---|---|---|---|---|
| 1 | 649.3512 | 28969 | 2764.8 | 2995076 | 100.0 | 0.0224 |
| 2 | 650.3538 | 30651 | 894.3 | 968144 | 32.3 | 0.0212 |
| 3 | 651.3493 | 28580 | 820.3 | 887268 | 29.6 | 0.0228 |
| 4 | 652.3516 | 22808 | 255.6 | 276312 | 9.2 | 0.0286 |

| Meas. m/z | # | Ion Formula | m/z | err [ppm] | mSigma | | Score | rdb | e⁻ Conf | N-Rule |
|---|---|---|---|---|---|---|---|---|---|---|
| 649.3512 | 1 | C38H46ClN8 | 649.3528 | 2.6 | 75.1 | 11 | 20.57 | 19.5 | even | ok |

**Fig. S3** HR-ESI-MS of Cy-Cl.

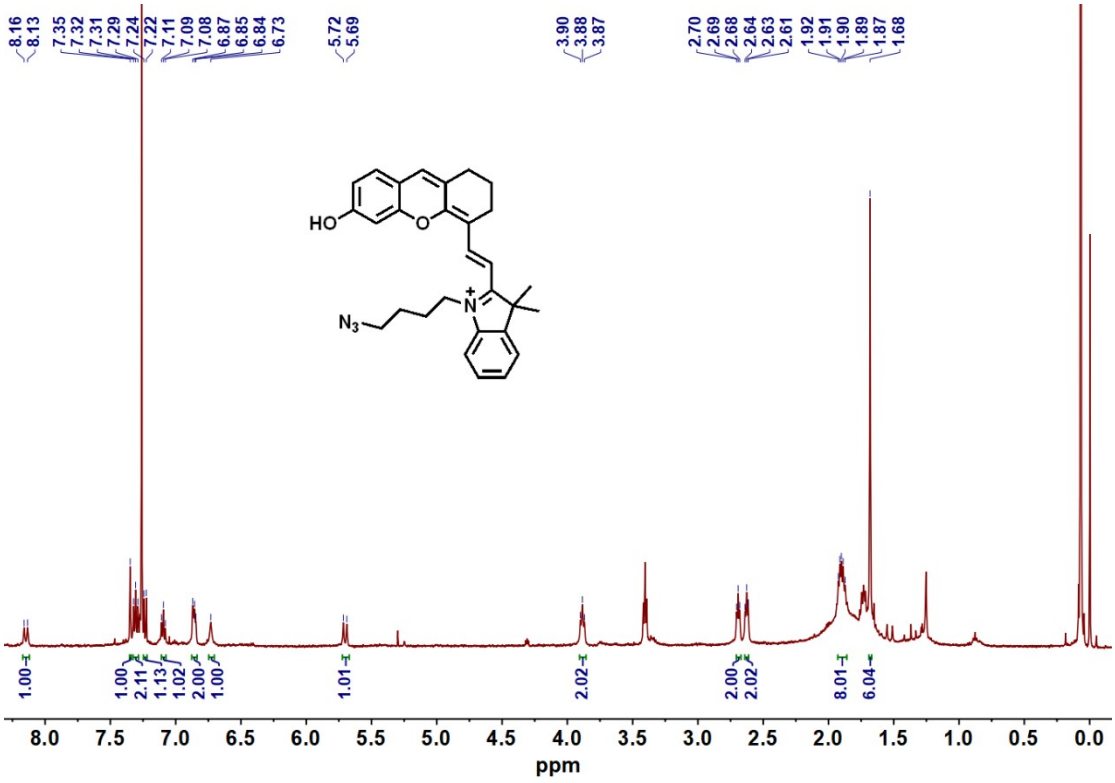


**Fig. S4** $^{1}$H NMR spectrum of CyOH in $CDCl_3$.

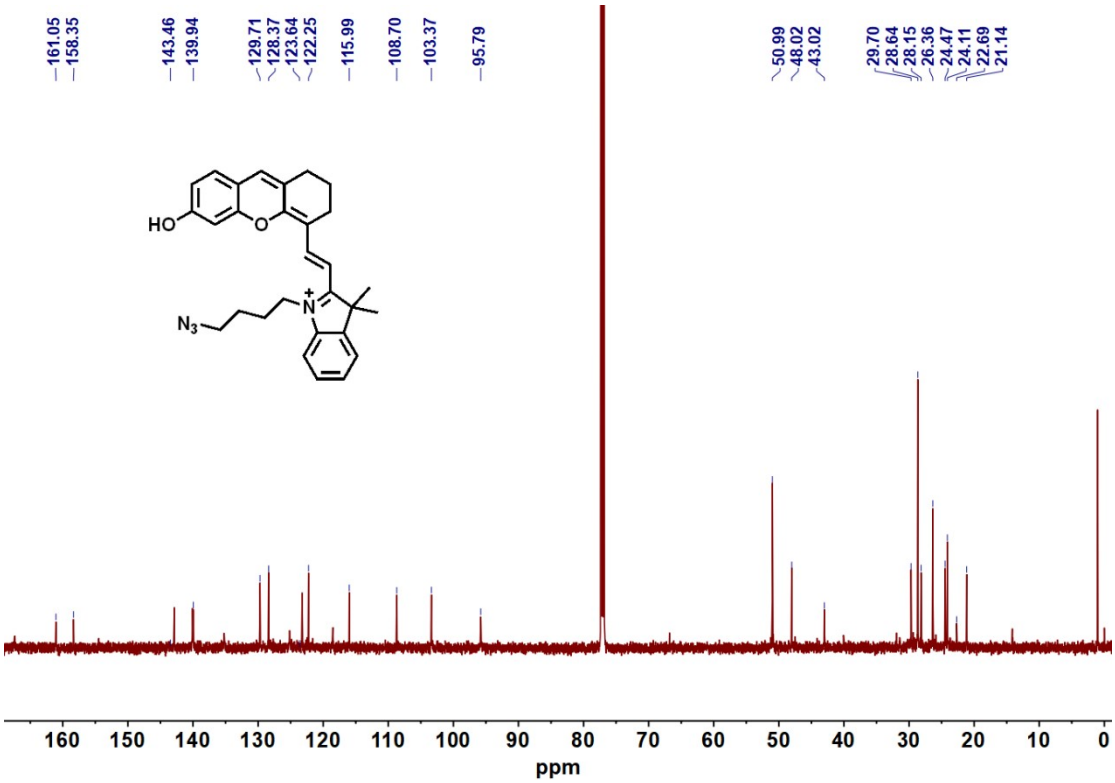


**Fig. S5** $^{13}C$ NMR of CyOH in $CDCl_3$.

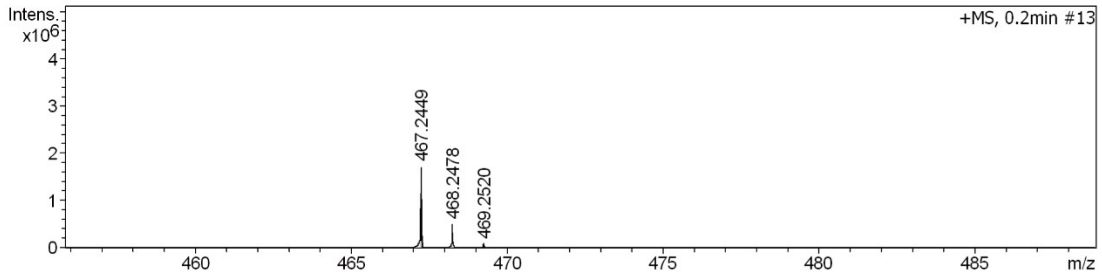


| # | m/z | Res. | S/N | I | I % | FWHM |
|---|---|---|---|---|---|---|
| 1 | 467.2449 | 35281 | 1797.0 | 1716472 | 100.0 | 0.0132 |
| 2 | 468.2478 | 28254 | 511.7 | 487828 | 28.4 | 0.0166 |
| 3 | 469.2520 | 19526 | 66.6 | 63368 | 3.7 | 0.0240 |

| Meas. m/z | # | Ion Formula | m/z | err [ppm] | mSigma | | Score | rdb | e¯ Conf | N-Rule |
|---|---|---|---|---|---|---|---|---|---|---|
| 467.2449 | 1 | C29H31N4O2 | 467.2442 | -1.6 | 26.4 | 1 | 100.00 | 16.5 | even | ok |

**Fig. S6** HR-ESI-MS of CyOH.

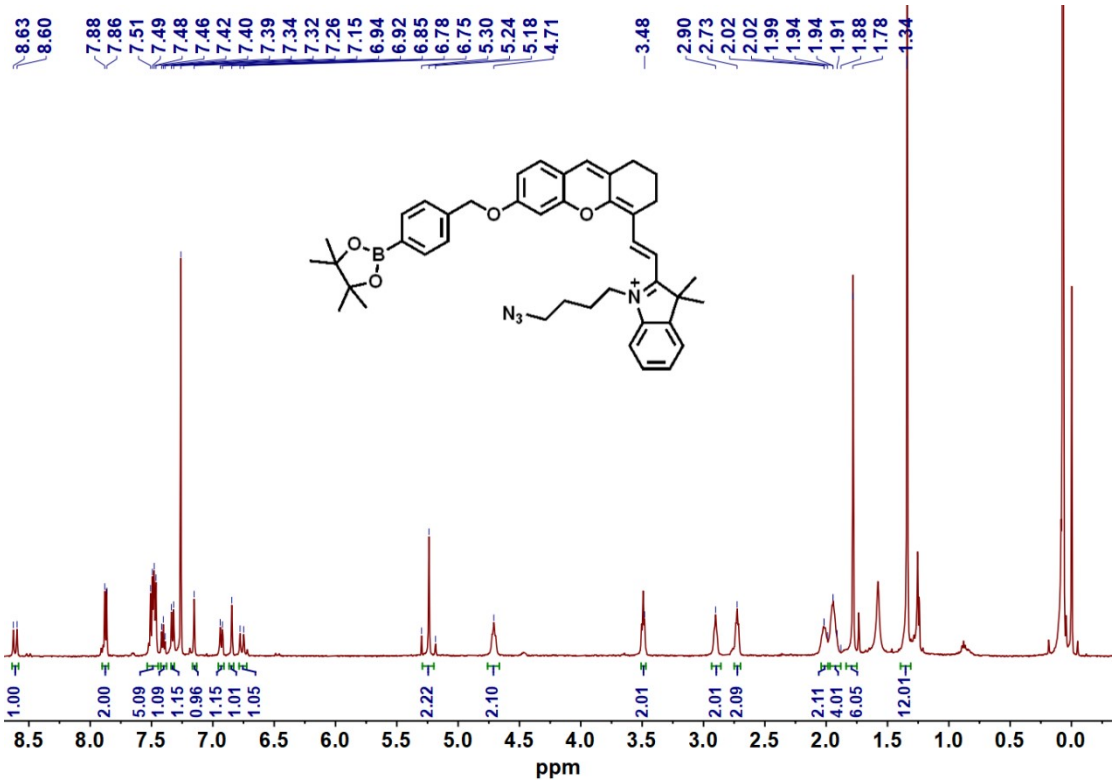


**Fig. S7** [1] H NMR spectrum of CyB in $CDCl_3$.

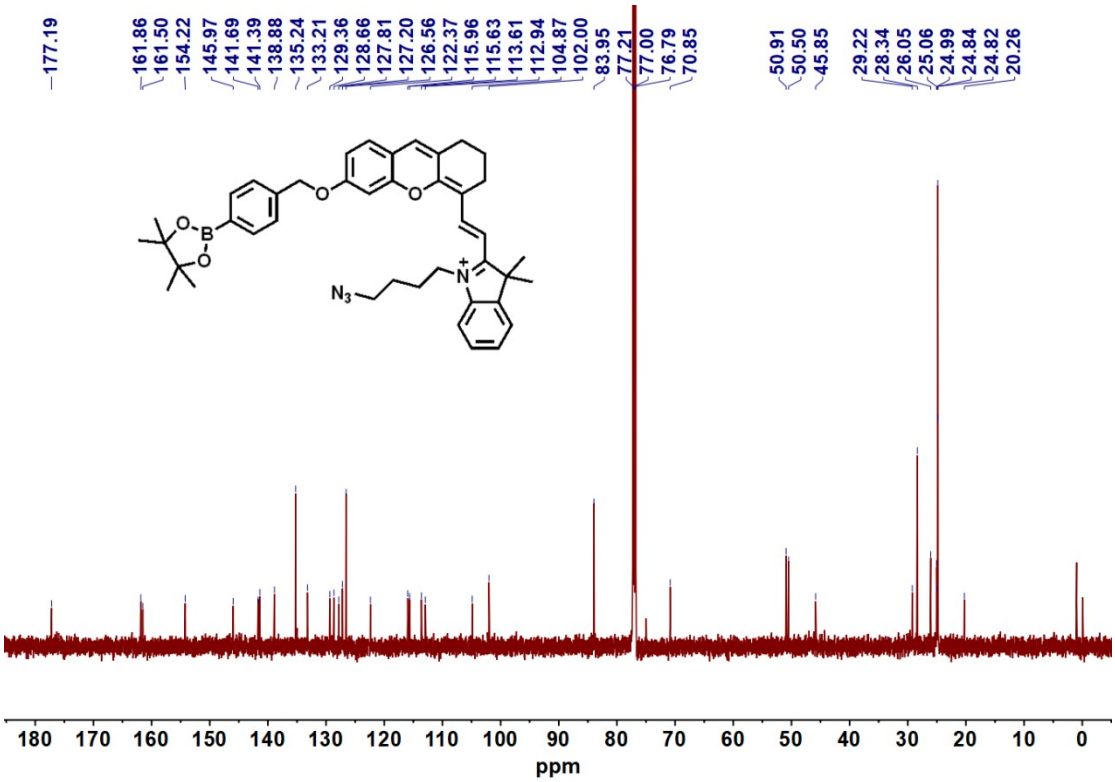


**Fig. S8** [13]C NMR of CyB in $CDCl_3$.

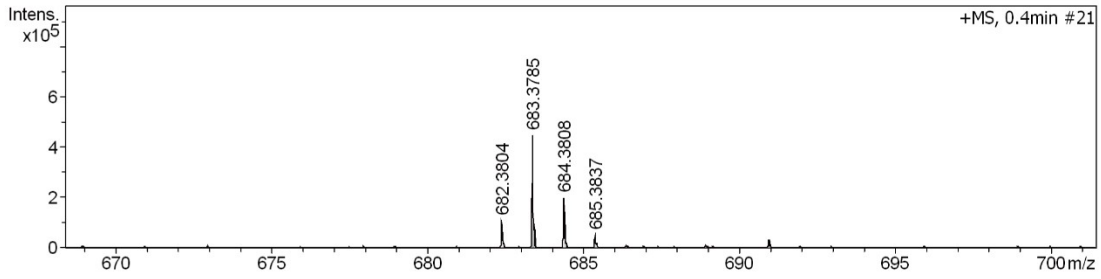


| # | m/z | Res. | S/N | I | I % | FWHM |
|---|---|---|---|---|---|---|
| 1 | 682.3804 | 20968 | 129.0 | 109932 | 24.7 | 0.0325 |
| 2 | 683.3785 | 23801 | 523.4 | 445728 | 100.0 | 0.0287 |
| 3 | 684.3808 | 20965 | 234.2 | 199152 | 44.7 | 0.0326 |
| 4 | 685.3837 | 17867 | 59.1 | 50236 | 11.3 | 0.0384 |

| Meas. m/z | # | Ion Formula | m/z | err [ppm] | mSigma | | Score | rdb | e¯ Conf | N-Rule |
|---|---|---|---|---|---|---|---|---|---|---|
| 683.3785 | 1 | C42H48BN4O4 | 683.3770 | -2.2 | 11.2 | 1 | 52.80 | 21.5 | even | ok |

**Fig. S9** HR-ESI-MS of CyB.

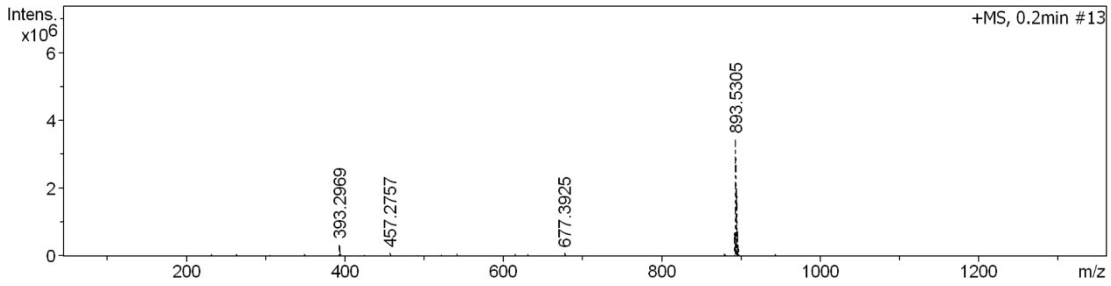


**Fig. S10** HR-ESI-MS of CyBT (Compounds is paramagnetic and can only be characterised by mass spectrometry).

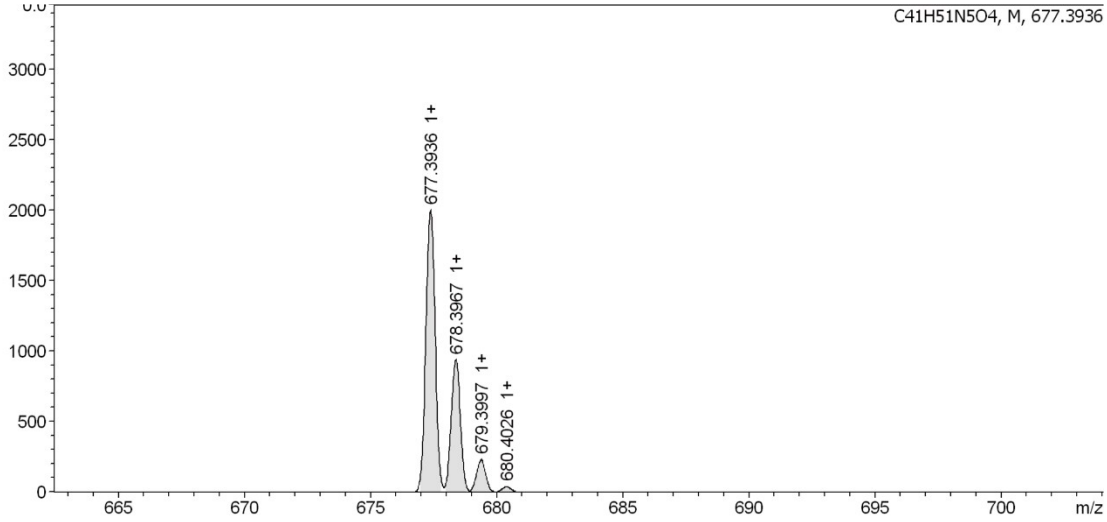


**Fig. S11** HR-ESI-MS of CyOT (Compounds is paramagnetic and can only be characterized by mass spectrometry).

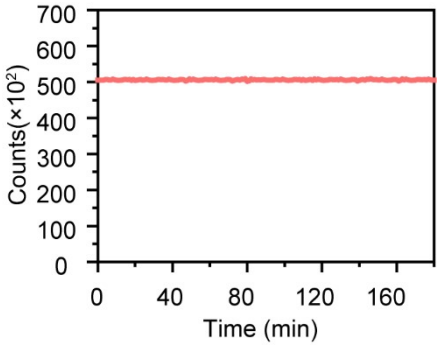


**Fig. S12** Photostability of CyBT in 10 mM pH 7.4 PBS solution after reaction with 10 μM $H_2O_2$.

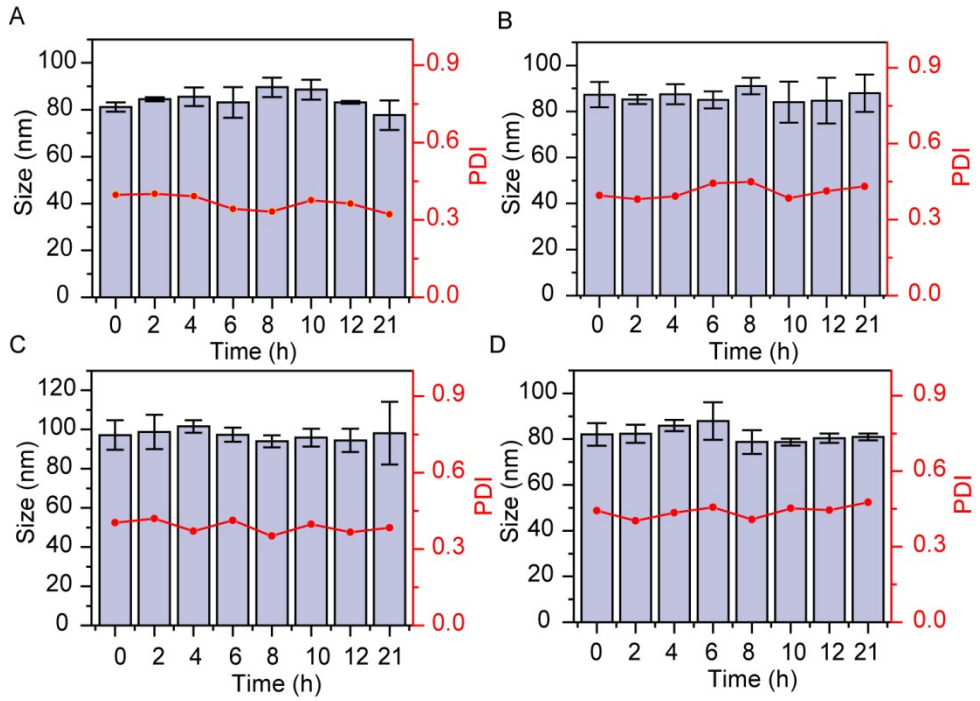


**Fig. S13** Particle size and PDI value of NPs-CyBT stored in PBS (A), water (B), normal saline (C), 10% FBS (D) for different time as determined by DLS measurement (mean±SD, n = 3).

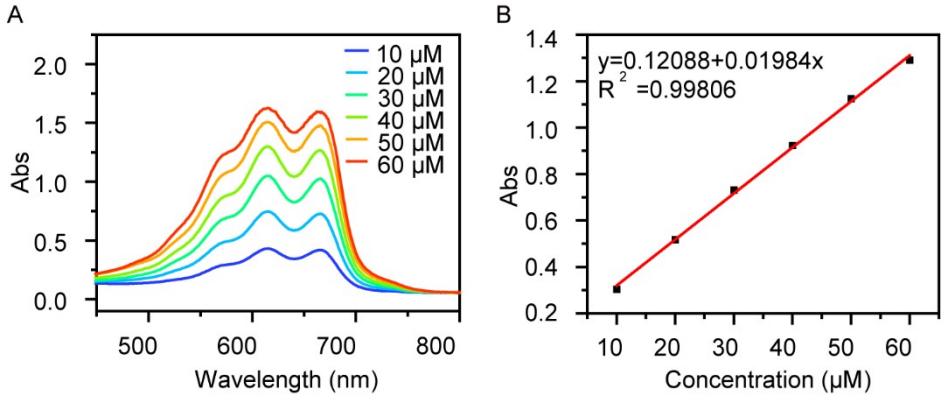


**Fig. S14** (A) Absorbance spectra of different concentrations of CyBT. (B) Standard curve of CyBT absorbance at 680 nm.

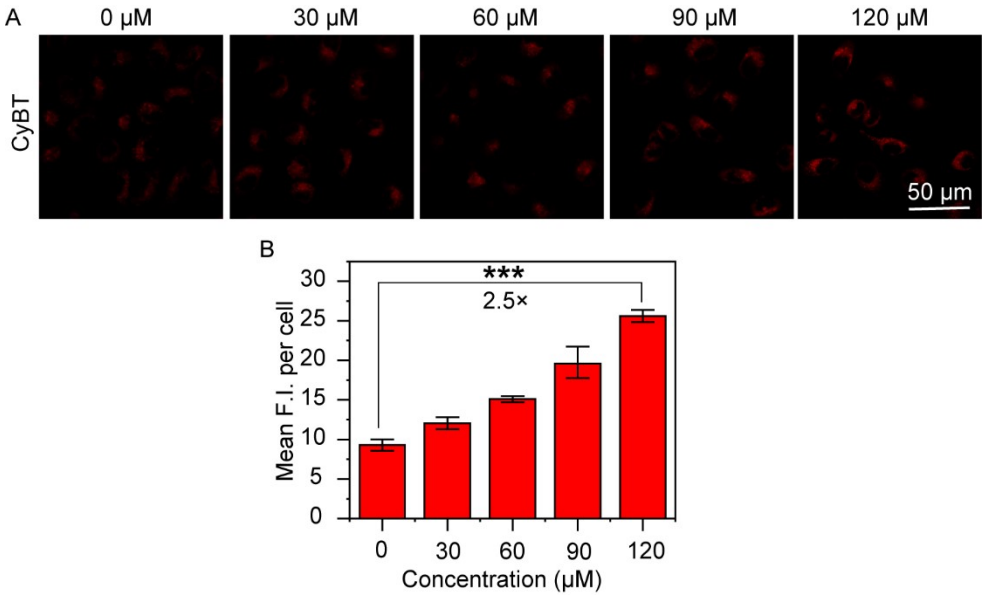


**Fig. S15** (A) Fluorescence images of exogenous $H_2O_2$ in HeLa cells by CyBT. The concentrations of $H_2O_2$ were 0, 30, 60, 90, 120 μM. (B) Histogram of the mean fluorescence intensity in (A) (mean±SD, n=3, *** p<=0.001).

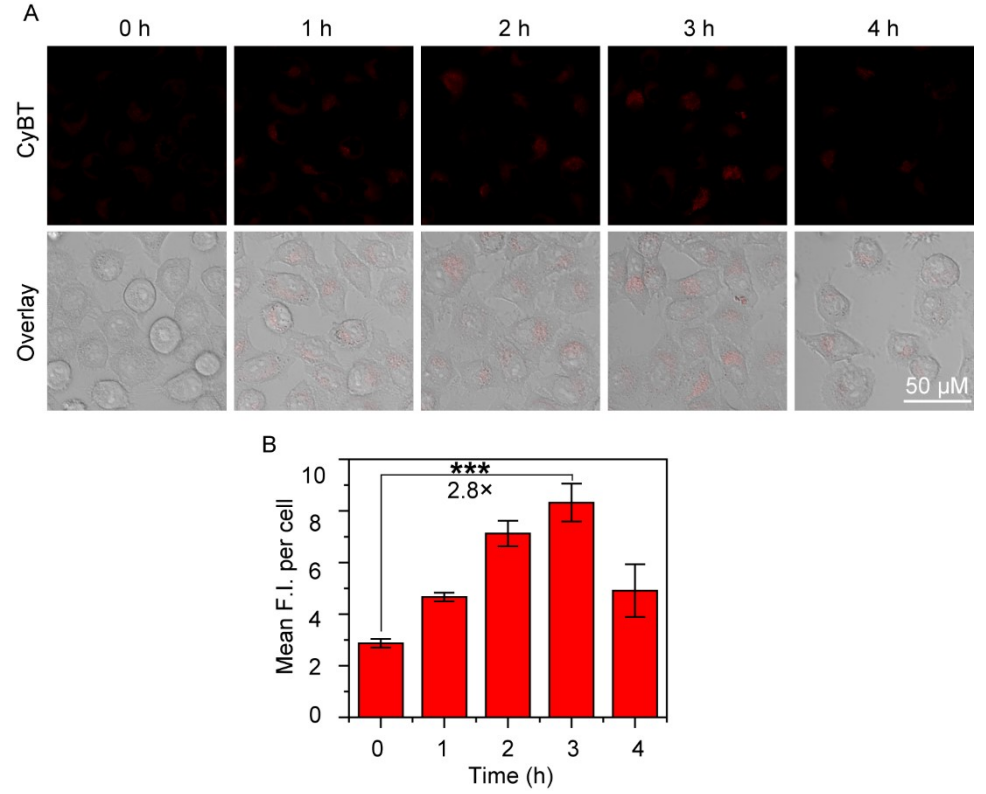


**Fig. S16** (A) Fluorescence imaging of cells incubated with CyBT at different time after X-ray irradiation. (B) Quantitative fluorescence analysis of cell imaging in (A) (mean±SD, n=3, *** p<=0.001).

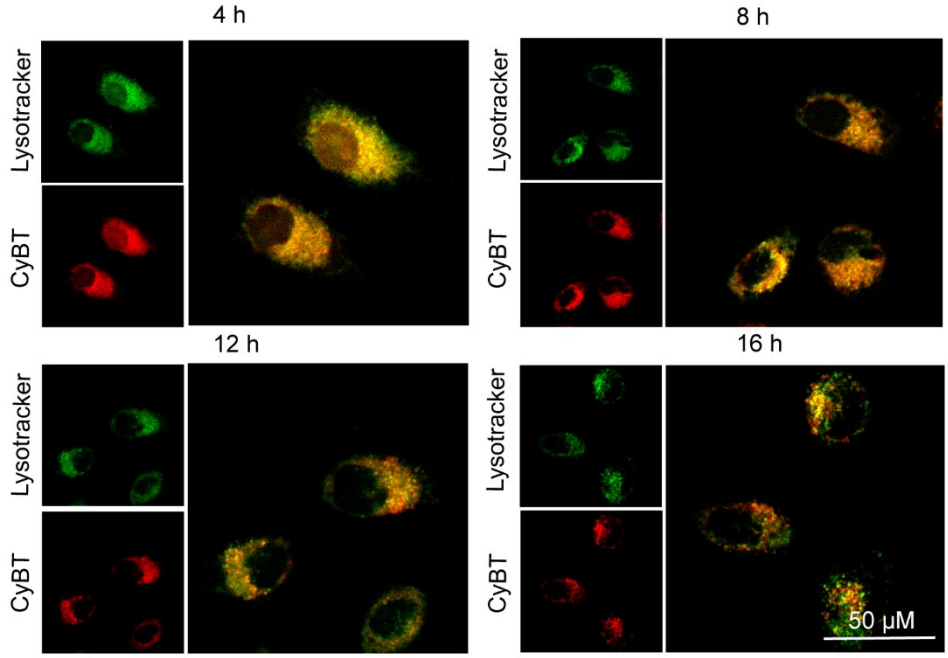


**Fig. S17** Co-localization imaging of NPs-CyBT with lysosomes in HeLa cells at different time.

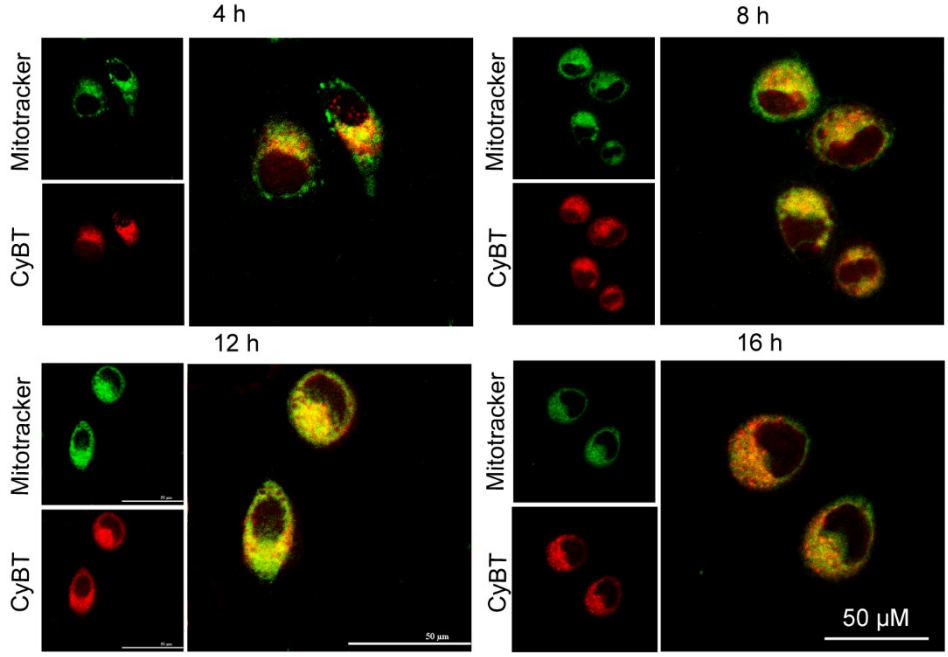


**Fig. S18** Co-localization imaging of NPs-CyBT with mitochondria in HeLa cells at different time.

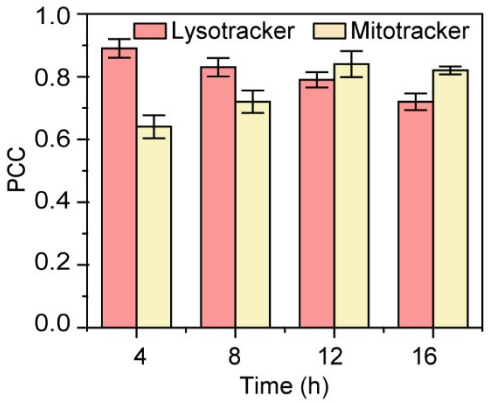


**Fig. S19** Pearson correlation coefficient changes in co-localisation imaging of NPs-CyBT with mitochondria and lysosome in HeLa cells over time (mean±SD).

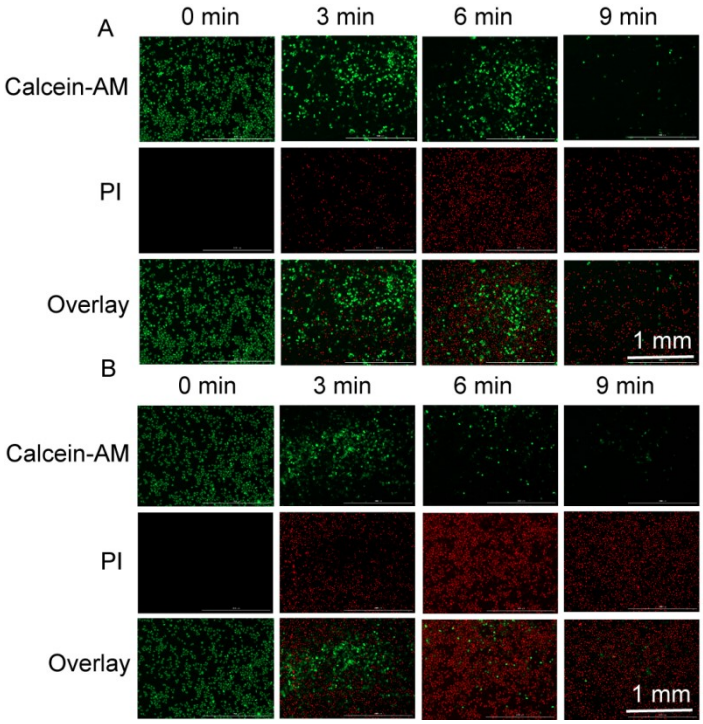


**Fig. S20** Live-dead staining imaging of cells pre-incubated with CyBT (A) and NPs-CyBT group (B) irradiated after irradiation with 655 nm laser.

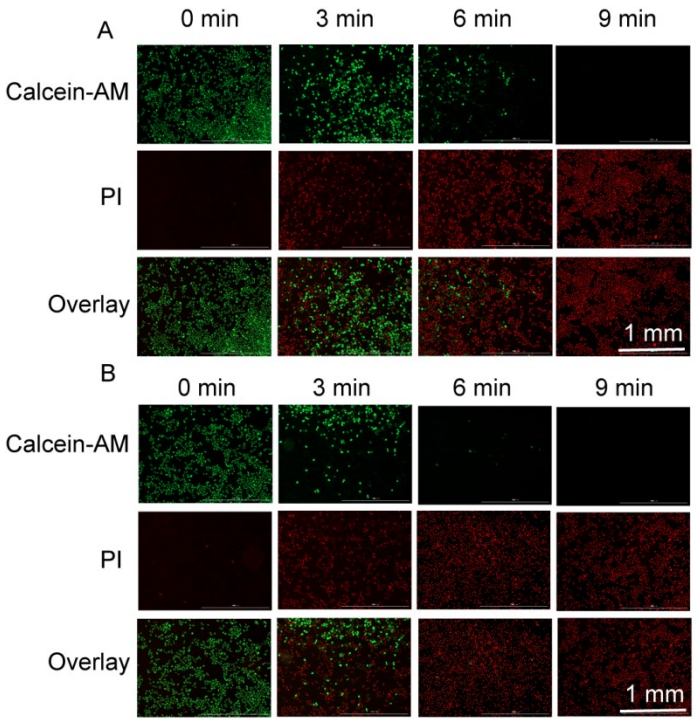


**Fig. S21** Live-dead staining imaging of cells pre-incubated with CyBT (A) and NPs-CyBT group (B) irradiated by X-ray followed by 655 nm laser irradiation.

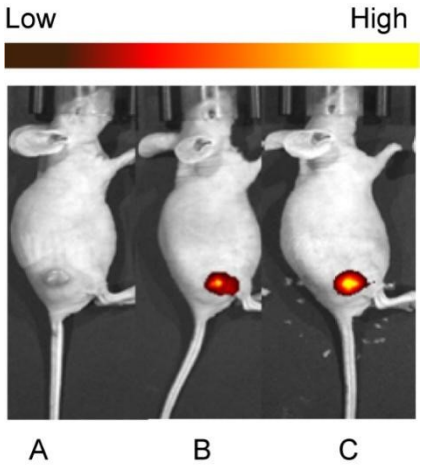


**Fig. S22** IVIS images of the HeLa tumor-bearing nude mice with i.t. injection from (A) PBS, (B) NPs-CyBT and (C) NPs-CyBT+X-Ray groups in 48 h ($\lambda_{ex}$= 680 nm, $\lambda_{em}$= 720 nm).

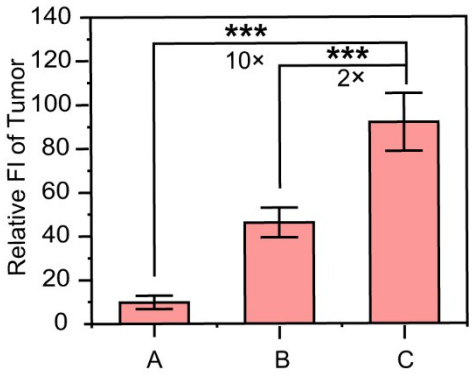


**Fig. S23** Histogram of the relative fluorescence intensity at tumor sites in Fig. S22 (mean±SD, n=3, *** p<=0.001).

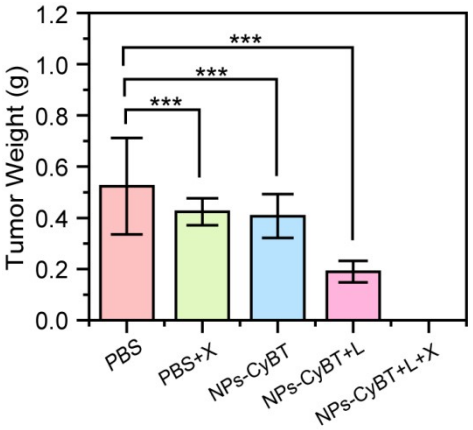


**Fig. S24** Average tumor weight of Hela tumor-bearing nude mice under specified treatment (mean±SD, n=5, *** p<=0.001).